

Structure of ERA in complex with the 3' end of 16S rRNA: Implications for ribosome biogenesis

Chao Tu, Xiaomei Zhou, Joseph E. Tropea, Brian P. Austin, David S. Waugh, Donald L. Court, and Xinhua Ji¹

Center for Cancer Research, National Cancer Institute, National Institutes of Health, Frederick, MD 21702

Edited by David R. Davies, National Institutes of Health, Bethesda, MD, and approved July 16, 2009 (received for review April 12, 2009)

ERA, composed of an N-terminal GTPase domain followed by an RNA-binding KH domain, is essential for bacterial cell viability. It binds to 16S rRNA and the 30S ribosomal subunit. However, its RNA-binding site, the functional relationship between the two domains, and its role in ribosome biogenesis remain unclear. We have determined two crystal structures of ERA, a binary complex with GDP and a ternary complex with a GTP-analog and the ₁₅₃₁AUCACCUCCUUA₁₅₄₂ sequence at the 3' end of 16S rRNA. In the ternary complex, the first nine of the 12 nucleotides are recognized by the protein. We show that GTP binding is a prerequisite for RNA recognition by ERA and that RNA recognition stimulates its GTP-hydrolyzing activity. Based on these and other data, we propose a functional cycle of ERA, suggesting that the protein serves as a chaperone for processing and maturation of 16S rRNA and a checkpoint for assembly of the 30S ribosomal subunit. The AUCA sequence is highly conserved among bacteria, archaea, and eukaryotes, whereas the CCUCC, known as the anti-Shine-Dalgarno sequence, is conserved in noneukaryotes only. Therefore, these data suggest a common mechanism for a highly conserved ERA function in all three kingdoms of life by recognizing the AUCA, with a "twist" for noneukaryotic ERA proteins by also recognizing the CCUCC.

GTPase | KH domain | 30S ribosomal subunit

The bacterial ribosome (70S) is composed of a large (50S) and a small (30S) subunit. The 30S ribosomal subunit (r-subunit) contains an approximately 1,540-nucleotide (nt) rRNA (16S rRNA) and 21 ribosomal proteins (r-proteins). The assembly of each r-subunit involves processing and maturation of rRNA, ordered binding of metal ions and r-proteins, and sequential conformational changes of the complex. Many proteins are associated with this process, including GTPases that represent the largest class of essential ribosome assembly factors in bacteria (1).

ERA is the first Ras-like small GTPase found in bacteria (2) and is essential for viability (3). ERA contains an N-terminal GTPase domain and a C-terminal KH domain. The structure of ligand-free *Escherichia coli* (Ec) ERA (apo-ERA) reveals that the GTPase domain resembles p21 Ras and the KH domain has a type-II fold (4). The structure of *Thermus thermophilus* (Tt) ERA in complex with the GTP analog GDPNP (ERA-GNP, PDB entry 1WF3) shows that the fold of TtERA is virtually identical to that of EcERA. The GTPase and KH domains are both essential for ERA function. However, the degree of interplay between the two domains, if any, remains unknown (5). ERA binds to 16S rRNA (6, 7) and the 30S r-subunit (8), and is believed to interact with a sequence near the 3' end of 16S rRNA (9, 10).

The 3' end of 16S rRNA plays important roles in the initiation of protein synthesis. For most mRNAs, selection of the correct start codon and translational reading frame is dependent on base pairing between the Shine-Dalgarno (SD) sequence (GGAGG) upstream from the initiator codon in the mRNA and the anti-SD sequence (₁₅₃₅CCUCC₁₅₃₉) near the 3' end of 16S rRNA (11, 12). Recently, the structure and dynamics of the SD/anti-SD interaction during translational initiation have been characterized (13). Here, we show that ERA binds to the ₁₅₃₁AUCACCUCCUUA₁₅₄₂ sequence at the 3' end of 16S rRNA and that the GTP-hydrolyzing activity of ERA increases upon binding of this 12-nt RNA. In an effort to further

understand of 16S rRNA maturation and ribosome biogenesis, we determined two crystal structures of ERA: a binary complex with GDP (ERA-GDP) and a ternary complex with GNP and the 12-nt RNA (ERA-GNP-RNA).

Results

Structural Overview. Four crystal structures have now been determined for ERAs from three bacteria: apo-ERA (PDB entry 1EGA) (4) and ERA-GDP (this work) from Ec; ERA-GNP from Tt (PDB entry 1WF3); and ERA-GNP-RNA from *Aquifex aeolicus* (Aa, this work). A structure-based sequence alignment reveals that the three ERAs share approximately 40% sequence identity (Fig. 1). The amino acid residue numbering of AaERA will be used hereafter unless otherwise stated.

The ERA-GNP-RNA structure includes a complete polypeptide chain of AaERA (amino acids 1–301) plus a nonnative His residue (amino acid 0, from cloning) at its N terminus, a Mg²⁺ ion, a GNP molecule, the first 11 nt of ₁₅₃₁AUCACCUCCUUA₁₅₄₂, and 245 water oxygens. The ERA-GDP structure reveals 2 incomplete chains of EcERA (amino acids 4–296), 2 GDP molecules, 13 sulfate ions, 1 Tris ion, and 42 water oxygens. The refinement statistics are summarized in Table S1. The GTPase domain consists of a central six-stranded β -sheet flanked by five α -helices, in which the GTP-binding site is located (Fig. S1). The two switch regions I and II of the GTPase domain are in contact with the bound GNP. The KH domain folds into a three-layered α - β - α sandwich with an RNA-binding groove on its surface. The GXXG loop ($\alpha 7$ – $\alpha 8$) and the variable loop ($\beta 7$ – $\beta 8$) of the KH domain interact with the bound RNA. The GTPase and KH domains are connected by a 17-amino acid linker.

Two Distinct Conformations. The 17-amino acid linker may enable dramatic changes to occur in the relative positions of the two domains, whereas the $\beta 9$ – $\alpha 9$ loop in the KH domain may allow large shifts of $\alpha 9$ with respect to the rest of the KH domain (Fig. S1). Nonetheless, the four structures display only two distinct conformations (Fig. 2A). ERA-GNP-RNA and ERA-GNP share conformation 1; the root-mean-square deviation (RMSD) for 257 out of 284 paired C α positions is 1.63 Å. ERA-GDP and apo-ERA share conformation 2; the RMSD for 284 out of 292 paired C α positions is 0.80 Å. Each conformation exhibits its own specific interactions between the two domains. In conformation 1, $\alpha 9$ wedges between $\beta 7$ of the KH domain and switch II of the GTPase domain (Fig. 2). In conformation 2, an interdomain β -sheet is formed between $\beta 7$ and βa (Fig. 2A). The βa strand is part of switch I (Fig. 1).

The four structures and two conformations of ERA (Fig. 2) offer

Author contributions: C.T., D.S.W., D.L.C., and X.J. designed research; C.T., X.Z., J.E.T., and B.P.A. performed research; C.T., X.Z., J.E.T., B.P.A., D.S.W., D.L.C., and X.J. analyzed data; and C.T. and X.J. wrote the paper.

The authors declare no conflict of interest.

This article is a PNAS Direct Submission.

Data deposition: The atomic coordinates and structure factors have been deposited in the Protein Data Bank, www.pdb.org (PDB ID codes 3IEU and 3IEV).

¹To whom correspondence should be addressed. E-mail: jix@ncicrf.gov.

This article contains supporting information online at www.pnas.org/cgi/content/full/0904032106/DCSupplemental.

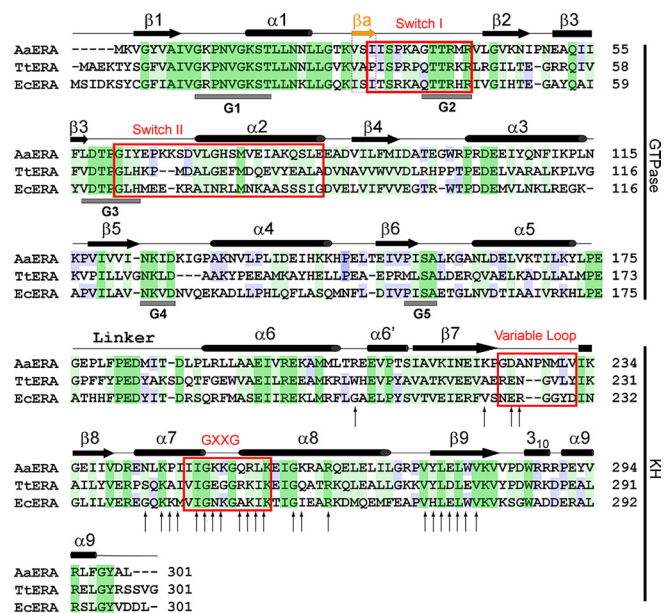


Fig. 1. Structure-based sequence alignment of AaERA, TtERA and EcERA (GenBank accession codes NP 214369, YP 143386 and YP 853700, respectively). Secondary structural elements and the position of the interdomain 17-aa linker are indicated above the sequences. The G1-G5 regions of the GTPase domain are indicated below the sequences. Switch regions I and II and the GXXG and variable loops are indicated. Identical residues and similar residues are shaded in dark and light green, respectively. Identical residues in any two of the three sequences are shaded in light blue. Residues in the ERA-GNP-RNA structure which interact with RNA are indicated with arrows. Detailed protein-RNA interactions are illustrated in Fig. S3.

an opportunity to examine the conformational changes of the protein in a stepwise manner. The fact that ERA-GNP-RNA and ERA-GNP share conformation 1 indicates that the binding of RNA does not elicit significant conformational changes in the protein. Similarly, the observation that ERA-GDP and apo-ERA share conformation 2 indicates that the release of GDP does not cause significant conformational changes. In contrast, GTP binding or hydrolysis causes dramatic conformational changes in the protein (Fig. 2B), as can be inferred from the two different conformational states.

Conformational Changes upon GTP Binding. Guanine nt molecules interact with highly conserved G protein regions G1-G5 of GTPases (14) (Fig. 1). In the ERA-GDP structure, GDP binds in a cavity created by G1, G4 and G5; the G2/switch I and G3/switch II regions, however, are distant from the guanine-nt-binding site (Fig. S2A). Upon GTP binding, multiple changes are observed. In the GTPase domain, the G2/switch I and G3/switch II regions are displaced by approximately 10 Å and 15 Å, respectively (Fig. 2B). Whereas the G2/switch I region serves as a ‘lid’ that covers the entire binding groove of the triphosphate moiety, the G3/switch II region interacts with the γ -phosphate only (Fig. S2B). With respect to the GTPase domain, the KH domain repositions itself by rotating extensively around the 17-amino acid linker and around its multiple internal axes (Fig. 2B). The detailed ERA-GNP interactions are illustrated (Fig. 3A).

Among the conformational changes in ERA that take place upon GTP binding, the relocation of $\alpha 9$ and disruption of the interdomain β -sheet appear to regulate the RNA-binding activity of ERA. The bound RNA is in contact with the GXXG and variable loops (Fig. 4A). The GXXG loop is relatively rigid, whereas the variable loop shows significant differences between the two conformations. In conformation 1, the variable loop together with the C terminus

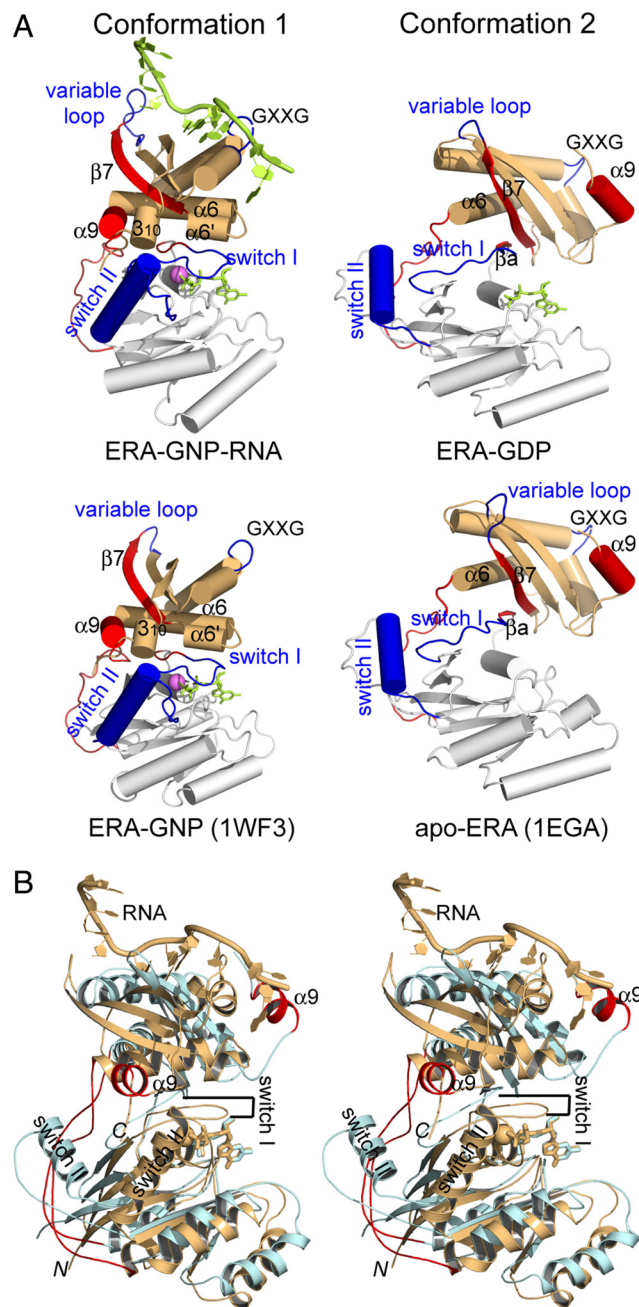


Fig. 2. Structure and conformation of ERA. (A) Four crystal structures are shown based on superimposed GTPase domains, including ERA-GNP-RNA (this work) and ERA-GNP (PDB entry 1WF3) sharing conformation 1, and apo-ERA (PDB entry 1EGA) and ERA-GDP (this work) sharing conformation 2. The color scheme is the same as in Fig. S1, except that the βa and $\beta 7$ strands are also highlighted in red. (B) Stereoview of superimposed ERA-GNP-RNA (in orange) and ERA-GDP (in cyan), showing dramatic differences between conformations 1 and 2.

of $\beta 7$ bends toward the RNA. This change appears to be internally regulated by the formation and breakage of the interdomain β -sheet between βa and $\beta 7$ (Fig. 2).

Unlike the conformational change in the variable loop, the relocation of $\alpha 9$ is dramatic (Fig. 4A). In conformation 1, $\alpha 9$ is far from RNA-binding site (Fig. 4B). In conformation 2, however, $\alpha 9$ packs against the surface formed by $\beta 7$, $\beta 8$, and $\beta 9$, creating a negatively-charged plateau that partially covers the RNA-binding surface (Fig. 4C).

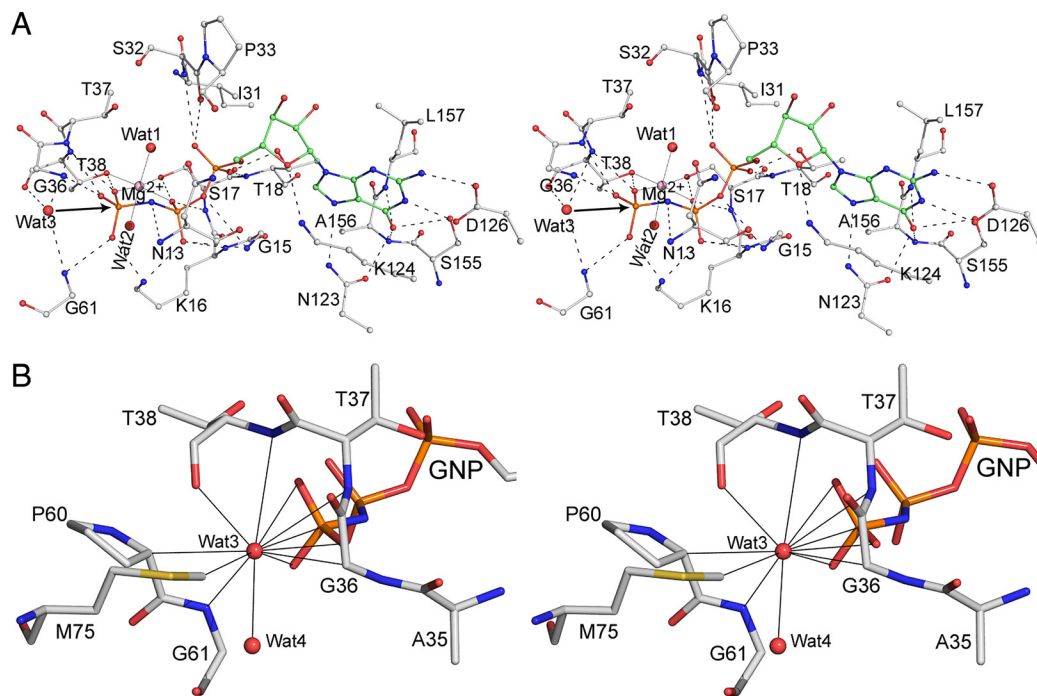


Fig. 3. ERA-GNP interactions in the ERA-GNP-RNA structure. (A) Stereoview showing the details of protein-GNP interactions. GNP is shown as a stick model in atomic colors (carbon, green; oxygen, red; nitrogen, blue; and phosphorus, orange). Amino acid residues are shown as stick models in the same atomic colors except that carbon is in gray. H-bonds are indicated with dashed lines. Three water molecules are shown and labeled as Wat1, Wat2, and Wat3, respectively. (B) Stereoview showing the details around Wat3. Schematic representation and color scheme are the same as in A. Distances less than or equal to 3.5 Å from Wat3 to neighboring atoms are indicated with thin, solid lines.

RNA Recognition. The ERA KH domain recognizes nt 1,531–1,539 in the ${}_{1531}\text{AUCACCUCCUUA}_{1542}$ sequence. The conformation of the bound RNA is dictated by seven anchor-point aa residues (Fig. 5). The RNA adopts a Z-like shape as it lies in a positively-charged groove. Eight out of the nine bases touch the bottom of the groove. Residues ${}_{1540}\text{UU}_{1541}$ make no contact with the KH domain and A1542 is not visible in the structure.

The ${}_{1531}\text{AUCA}_{1534}$ sequence winds around two lysine side chains in the GXXG (XX = ${}_{251}\text{KK}_{252}$ in AaERA) loop (Fig. 5); the specificity for this sequence is primarily mediated by interactions between nt bases and aa main-chain groups (Fig. S3A). A1531 is recognized by a Watson-Crick-like (WCL) base pairing between main-chain atoms of R207 and the adenine base. U1532 exhibits two conformations, in one of which the uridine base is recognized by the main-chain carbonyl of N243. The C1533 base is recognized by the side chain of conserved K245. Like A1531, A1534 is also recognized by WCL hydrogen (H-) bonds between the adenine base and main-chain atoms of V281. Additional hydrophobic interactions and water-mediated H-bonds are also observed between the RNA and the protein (Fig. S3A).

The ${}_{1535}\text{CCUCC}_{1539}$ sequence makes contact with $\alpha 8$ and $\beta 9$ as well as the variable loop of ERA (Fig. 5). Four out of five bases are recognized by amino acid main-chain groups (Fig. S3B). C1535 is recognized via a H-bond (2.71 Å) between atom N4 of the base and carbonyl of L279. The N4 atom of the C1536 base forms a H-bond with carbonyl of G260, whereas O2 and N3 form WCL H-bonds with side-chain atoms of conserved R264. The uridine of U1537 also engages in WCL base pairing with main-chain atoms of L277. Furthermore, there are triple π - π interactions between the C1536 and U1537 bases and the side chain of Y276 (Y273 in TtERA, H274 in EcERA). The RNA then makes a sharp ($\sim 90^\circ$) turn between U1537 and C1538 (Fig. 5). The C1538 base forms H-bonds with the backbone amide group of D225 and side-chains of E278 (D in Tt, E in Ec) and K222. The base of C1539 engages in π - π stacking

interactions with C1538, U1540, and U1541 as well as a water-mediated H-bond with the side chain of Y276 (Y in Tt, H in Ec).

In summary, the recognition of the 9-nt RNA by ERA involves 19 H-bonds, including (i) 10 H-bonds between amino acid main-chain groups and the bases of nt A1531, U1532, A1534, C1535, C1536, U1537, and C1538, (ii) three H-bonds between the side chains of strictly conserved K245 and R264 and the bases of C1533 and C1536, (iii) three H-bonds between the main-chain groups of residues 225, 226, and 275 and the 2'-hydroxyl groups of U1537 and C1538 (Fig. S3C), (iv) two H-bonds between the side chains of D225 (E in Tt and Ec) and R255 (K in Tt and Ec) and the 2'-hydroxyl groups of A1531 and C1539, and (v) a H-bond between the side chain of E278 (D in Tt, E in Ec) and the C1538 base. Nonconserved K222 also forms a H-bond with the C1538 base (Fig. S3C), which may contribute to a minor difference in RNA recognition by ERA in different bacteria.

RNA Recognition Stimulates GTP-Hydrolyzing Activity. The intrinsic GTP-hydrolyzing activity of Ras is low (15), but can be accelerated $>10^5$ -fold by GAP (16, 17). The intrinsic GTP-hydrolyzing activity of ERA is also low (18), ranging from 0.01 to 0.02 $\text{mmol min}^{-1} \text{mmol}^{-1}$, but is stimulated 3- to 12-fold in the presence of 16S rRNA (6, 7). We believe that 16S rRNA plays a GAP-like role by accelerating the GTP-hydrolyzing activity of ERA, and we have tested whether the 12-nt RNA can do so. A GTPase assay used for ERA in the presence or absence of the RNA shows that it indeed stimulates the activity. The specific activities of AaERA in the absence or presence of RNA are 0.02 and 0.11 $\text{mmol min}^{-1} \text{mmol}^{-1}$ (~ 6 -fold higher), respectively. The degree of Ras stimulation by GAP is much larger than that of ERA stimulation by RNA, which is likely because of differing mechanisms of stimulation (See Discussion for details).

Our results also show that each of the ${}_{1531}\text{AUCA}_{1534}$ and ${}_{1535}\text{CCUCC}_{1539}$ sequences impacts the GTP-hydrolyzing activity

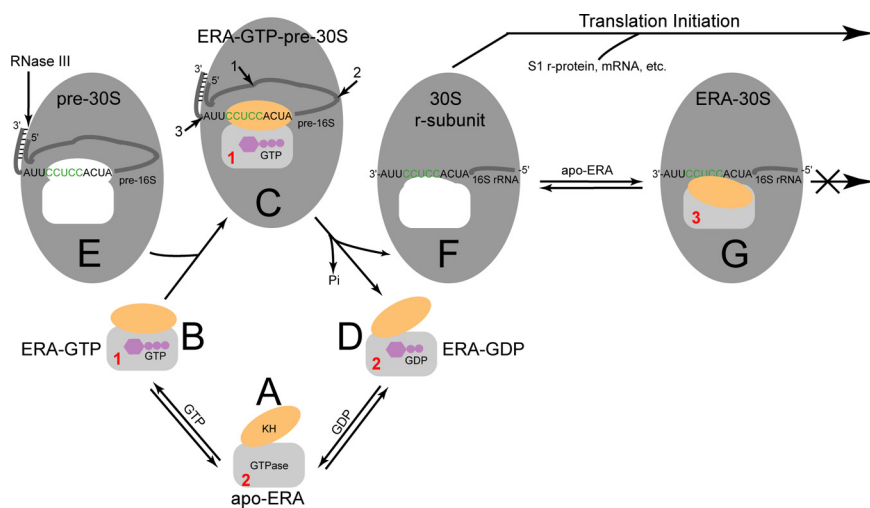


Fig. 6. Schematic illustration for the functional cycle of ERA. The GTPase domain is represented by a gray rectangle, the KH domain by an orange oval, GTP and GDP by purple cartoons, and the conformations of ERA by numbers in red. The pre-30S particle and 30S r-subunit are represented by larger gray ovals. The pre-16S rRNA (an RNase III cleavage product with a 26-bp stem and a 2-nt 3' overhang as indicated) and 16S rRNA are represented by a gray line with embedded ${}_{1531}\text{AUCACCUCCUUA}_{1542}$ sequence at the 3' end. The unoccupied ERA-binding pocket in the pre-30S particle and that in the 30S r-subunit are indicated in white. The four functional states, including (A) apo-ERA, (B) ERA-GTP, (C) ERA-GTP-pre-30S, and (D) ERA-GDP, are represented by the apo-ERA (PDB entry 1EGA), ERA-GNP (PDB entry 1WFF3), ERA-GNP-RNA (this work), and ERA-GDP (this work) structures. In C, the cleavage sites of RNase E, RNase G and the unknown nuclease are indicated with numbered arrows 1, 2 and 3, respectively. (E) The pre-30S particle contains pre-16S rRNA. (F) The mature 30S r-subunit contains 16S rRNA. (G) The mature 30S r-subunit may bind apo-ERA in a distinct conformation 3 (PDB entry 1X1L).

nomenon in physics where a water molecule is pushed away from a hydrophobic surface (27). Therefore, ERA-catalyzed GTP hydrolysis follows a substrate-assisted mechanism (28) by which GTP acts as a general base, the γ -phosphate of GTP is protonated by Wat3, and no other factor is required. Third, the exchange of the Ras-bound GDP for GTP requires a guanine-nt exchange factor (GEF) (29), whereas the ERA-bound GDP can easily exchange with GTP and vice versa (30). In order words, the GDP- and GTP-bound forms of ERA exist in a rapid equilibrium, the net effect of which is lowered GTP hydrolysis. RNA recognition by ERA may stabilize the ERA-GTP complex and thus increase the efficiency and/or turnover of GTP hydrolysis by the protein. Additionally, other as yet undiscovered protein-ERA and/or protein-RNA interactions in the ERA-GTP-pre-30S complex may participate in the stimulation of GTP hydrolysis.

Functional Cycle of ERA. RNase III cleaves the primary rRNA transcript and produces precursor 16S rRNA (pre-16S rRNA) that features a 26-base pair (bp) stem (31). ERA is required to convert pre-16S rRNA into 16S rRNA (8, 32), during which 115 nt are removed from the 5' end by RNase E and RNase G, whereas 33 nt are removed from the 3' end by an unknown RNase (33, 34). The ${}_{1531}\text{AUCACCUCC}_{1539}$ sequence is only 3 nt away from the cleavage site of the unknown RNase.

Considering four ERA structures in four states (Fig. 2), we propose the following functional cycle of the protein during processing and maturation of 16S rRNA (Fig. 6). Apo-ERA assumes conformation 2 (Fig. 6A). The binding of GTP causes dramatic conformational changes in the protein, and ERA-GTP adopts conformation 1 (Fig. 6B). The binding of pre-16S rRNA (Fig. 6E) by ERA-GTP (Fig. 6B), leading to the formation of ERA-GTP-pre-30S (Fig. 6C), does not cause significant conformational changes in ERA. Nonetheless, the recognition of the ${}_{1531}\text{AUCACCUCC}_{1539}$ sequence by the protein stimulates its GTP-hydrolyzing activity and may also signal the final processing of 16S rRNA by RNase E, RNase G, and the unknown RNase (Fig. 6C). In concert with the final processing, the completion of GTP hydrolysis triggers the dramatic conformational change of ERA from conformation 1 back to conformation 2, which should be sufficient to facilitate the departure of ERA-GDP (Fig. 6D) from the mature 30S r-subunit (Fig. 6F). The rate of guanine nt release by ERA is rapid (30), and thus, GDP is released without the aid of a GEF (Fig. 6A). The rate of guanine nt association by ERA is also rapid, especially in the presence of magnesium (30). The concentration of GTP in the cell

is higher than that of GDP, and therefore, ERA-GTP (Fig. 6A) is readily available for the next functional cycle.

The mature 30S r-subunit (Fig. 6F) is ready for translation initiation. However, it may also bind apo-ERA to form an ERA-30S complex (Fig. 6G), locking the 30S r-subunit in a conformation that is not favorable for association with the 50S r-subunit (10). According to a cryo-electron microscopy (cryo-EM) image constructed by Sharma and coworkers (10), neither conformation 1 (ERA-GTP, Fig. 6B) nor conformation 2 (ERA-GDP, Fig. 6D) of ERA is compatible with the ERA-binding cavity in the mature 30S r-subunit (Fig. 6F). Further, docking of ERA into the cavity (Fig. 6G) would require dramatic conformational changes that obscure its GTP-binding pocket (Fig. S5). This implies the existence of a third conformation for ERA (conformation 3) when it binds to the mature 30S r-subunit, and the collapsed GTP-binding pocket indicates that only apo-ERA can bind to the mature 30S r-subunit. In fact, addition of GTP or GDP precludes ERA binding to the mature 30S r-subunit (8). Whether apo-ERA can assume conformation 3 when it is not embedded in the 30S r-subunit remains to be determined.

ERA and Ribosome Biogenesis. ERA is required for the maturation of 16S rRNA (8, 32). It recognizes the ${}_{1531}\text{AUCACCUCC}_{1539}$ sequence that is very close to the mature 3' end of 16S rRNA, raising the possibility that ERA binding may protect the AUCACCUCC sequence from accidental damage during maturation by, for example, the unknown RNase (Fig. 6C). In addition, ERA binding may change the conformation of pre-16S rRNA to assist RNases in processing and facilitate the activity of other factors, such as KsgA. KsgA methylates two adjacent adenosine residues in the last helix (helix 45, residues 1,507–1,528) near the 3' end of 16S rRNA (35–37). The methylation occurs at a later stage of processing and maturation of 16S rRNA but before the 30S r-subunit becomes competent to initiate translation (35–37). ERA binds to pre-16S when it is complexed with GTP and releases mature 16S upon the completion of GTP hydrolysis. We believe, therefore, that ERA acts as a chaperone for processing and maturation of 16S rRNA.

The selection of the correct initiation codon and translational reading frame in an mRNA depends on base pairing between the SD sequence (GGAGG) located upstream of the initiator codon and the anti-SD sequence CCUCC (11, 12). The binding of the AUCACCUCC sequence by ERA prevents base pairing between the anti-SD and SD sequences, thereby preventing mRNA recruitment to the pre-30S particle. In light of the fact that the ERA-binding site on the 30S significantly overlaps with that of the S1 r-protein (10), which is known to directly affect the SD/anti-SD

interaction (38, 39), the binding of 16S rRNA by ERA would also occlude the binding of S1. Thus, the initiation of mRNA translation by the 30S r-subunit would seem to be possible only after ERA is released, suggesting that ERA functions as a checkpoint for ribosome assembly and final activation of the mature 30S r-subunit.

Materials and Methods

Cloning, Protein Expression and Purification. EcERA was prepared as described (18, 40). To prepare AaERA, the ORF (ORF) encoding the protein was amplified from genomic DNA by PCR. The PCR amplicon was subsequently used as template for a second PCR. The amplicon from the second PCR was inserted into the entry vector pDONR201 (Invitrogen) and the nucleotide sequence was confirmed. The ORF, encoding the His₆-ERA gene with a recognition site for tobacco etch virus (TEV) protease (ENLYFQ/G) fused in-frame to its N terminus, was moved into the destination vector pKM596 to produce pBA1971. The pBA1971 directs the expression of AaERA as a fusion to the C terminus of *E. coli* maltose-binding protein with an intervening TEV protease recognition site so that upon cleavage, AaERA retains an N-terminal hexahistidine tag. The fusion protein was expressed in *E. coli* strain BL21-CodonPlus (DE3)-RIL (Stratagene). The purification was performed at 4–8°C. Details for the preparation of AaERA are described in *SI Text*.

RNA Oligos. The ¹⁵³¹AUCACCUCCUUA¹⁵⁴² sequence was derived from the 3' end of *E. coli* 16S rRNA, corresponding to the AUCACCUCCUUU sequence in the *A. aeolicus* 16S rRNA. The RNA' (¹⁵³¹AUCAGGAGGUUA¹⁵⁴²) and RNA'' (¹⁵³¹UAGUC-CUCCUUA¹⁵⁴²) were designed by replacing either the anti-SD (CCUCC) or the highly conserved (AUCA) sequence with its complementary sequence. The three RNA oligos were purchased (Integrated DNA Technologies) and used without further purification.

GTP-Hydrolyzing Activity. The assay was performed according to the protocol provided by the GTPase assay kit (high sensitivity; Innova Biosciences). The measurement of free phosphate (P_i) was based on the change in absorbance of malachite green in the presence of molybdate. 100 μL AaERA (0.024 mM) mixed

with different RNA (molar ratio 1:1.5) were incubated at 37°C for 30 min with 100 μL substrate-buffer mix containing 0.5 mM purified GTP (final concentration), 60 mM Tris (pH 7.5), 3.75 mM MgCl₂, and 100 mM NaCl. After incubation, 50 μL P_i-ColorLock Gold mix (containing 5 M HCl) was added to stop the reactions. 20 μL stabilizers were added after 2 min. The mixtures were read at 635 nm after sitting at 37°C for 30 min. A standard curve was derived according to the provided protocol for calculating the specific activity of ERA. Each experiment was repeated three times. The specific activity of ERA was calculated according to the equation: Activity = (A × C) / 500B, where, A = concentration of P_i (μM) determined from the standard curve, B = assay time in minutes, C = reciprocal of the enzyme dilution factor.

Crystal Structure Determination. Crystals of EcERA-GDP were grown at 15 ± 1°C using hanging-drop vapor diffusion. Diffraction data were collected at beamline X9B of the National Synchrotron Light Source (NSLS), Brookhaven National Laboratory. Crystals of AaERA-GNP-RNA were grown at 19 ± 1°C. A Hydra II Plus One (Matrix Technologies Corporation) crystallization robot was used. Data were collected at beam line 22-BM of the Southeast Regional Collaborative Access Team (SER-CAT) at the Advanced Photon Source (APS), Argonne National Laboratory. Crystal data and processing statistics are summarized in *Table S1*.

The ERA-GDP structure was determined by Fourier synthesis, whereas the ERA-GNP-RNA was solved by molecular replacement. For refinement, bulk solvent correction was used. Electron density maps were calculated for inspection and improvement of the structures. Ligands and water molecules were added at later stages of the refinement. Illustrations were prepared with PyMOL (DeLano Scientific LLC). Details of structure determination and validation are described in *SI Text*.

ACKNOWLEDGMENTS. We thank Drs. M. Bubunenko, X. Chen, Y. Gu, and W. Guo for help and Drs. M. Bubunenko, J. Strathern, and A. Wlodawer for reading the manuscript. Diffraction data were collected at X9B, NSLS, Brookhaven National Laboratory and 22-BM (SER-CAT), APS, Argonne National Laboratory. This work was supported by the Intramural Research Program of the National Institutes of Health, National Cancer Institute, Center for Cancer Research.

- Karbstein K (2007) Role of GTPases in ribosome assembly. *Biopolymers* 87:1–11.
- Ahn J, March PE, Takiff HE, Inouye M (1986) A GTP-binding protein of *Escherichia coli* has homology to yeast RAS proteins. *Proc Natl Acad Sci USA* 83:8849–8853.
- Takiff HE, Chen SM, Court DL (1989) Genetic analysis of the *mc* operon of *Escherichia coli*. *J Bacteriol* 171:2581–2590.
- Chen X, Court DL, Ji X (1999) Crystal structure of ERA: A GTPase-dependent cell cycle regulator containing an RNA binding motif. *Proc Natl Acad Sci USA* 96:8396–8410.
- Hang JQ, Zhao GS (2003) Characterization of the 16S rRNA- and membrane-binding domains of *Streptococcus pneumoniae* Era GTPase - Structural and functional implications. *Eur J Biochem* 270:4164–4172.
- Meier TI, Peery RB, Jaskunas SR, Zhao G (1999) 16S rRNA is bound to era of *Streptococcus pneumoniae*. *J Bacteriol* 181:5242–5249.
- Meier TI, Peery RB, McAllister KA, Zhao G (2000) Era GTPase of *Escherichia coli*: Binding to 16S rRNA and modulation of GTPase activity by RNA and carbohydrates. *Microbiology* 146:1071–1083.
- Sayed A, Matsuyama S, Inouye M (1999) Era, an essential *Escherichia coli* small G-protein, binds to the 30S ribosomal subunit. *Biochem Biophys Res Commun* 264:51–54.
- Lu Q, Inouye M (1998) The gene for 16S rRNA methyltransferase (ksgA) functions as a multicopy suppressor for a cold-sensitive mutant of era, an essential RAS-like GTP-binding protein in *Escherichia coli*. *J Bacteriol* 180:5243–5246.
- Sharma MR, et al. (2005) Interaction of Era with the 30S ribosomal subunit implications for 30S subunit assembly. *Mol Cell* 18:319–329.
- Gold L, et al. (1981) Translational initiation in prokaryotes. *Annu Rev Microbiol* 35:365–403.
- Shine J, Dalgarno L (1974) The 3'-terminal sequence of *Escherichia coli* 16S ribosomal RNA: Complementarity to nonsense triplets and ribosome binding sites. *Proc Natl Acad Sci USA* 71:1342–1346.
- Korostelev A, et al. (2007) Interactions and dynamics of the Shine Dalgarno helix in the 70S ribosome. *Proc Natl Acad Sci USA* 104:16840–16843.
- Sprang SR (1997) G protein mechanisms: Insights from structural analysis. *Annu Rev Biochem* 66:639–678.
- Bollag G, McCormick F (1995) Intrinsic and GTPase-activating protein-stimulated Ras GTPase assays. *Methods Enzymol* 255:161–170.
- Ahmadian MR, Hoffmann U, Goody RS, Wittlinghofer A (1997) Individual rate constants for the interaction of Ras proteins with GTPase-activating proteins determined by fluorescence spectroscopy. *Biochemistry* 36:4535–4541.
- Gideon P, et al. (1992) Mutational and kinetic analyses of the GTPase-activating protein (GAP)-p21 interaction: The C-terminal domain of GAP is not sufficient for full activity. *Mol Cell Biol* 12:2050–2056.
- Chen SM, et al. (1990) Expression and characterization of RNase III and Era proteins. Products of the *mc* operon of *Escherichia coli*. *J Biol Chem* 265:2888–2895.
- Raué HA, Klootwijk J, Musters W (1988) Evolutionary conservation of structure and function of high molecular weight ribosomal RNA. *Prog Biophys Mol Biol* 51:77–129.
- Neefs JM, Van de Peer Y, Hendriks L, De Wachter R (1990) Compilation of small ribosomal subunit RNA sequences. *Nucleic Acids Res* 18:2237–2317.
- Grishin NV (2001) KH domain: One motif, two folds. *Nucleic Acids Res* 29:638–643.
- Beuth B, Pennell S, Arnvig KB, Martin SR, Taylor IA (2005) Structure of a *Mycobacterium tuberculosis* NusA-RNA complex. *EMBO J* 24:3576–3587.
- Lewis HA, et al. (2000) Sequence-specific RNA binding by a Nova KH domain: Implications for paraneoplastic disease and the fragile X syndrome. *Cell* 100:323–332.
- Liu ZH, et al. (2001) Structural basis for recognition of the intron branch site RNA by splicing factor 1. *Science* 294:1098–1102.
- Valverde R, Edwards L, Regan L (2008) Structure and function of KH domains. *FEBS J* 275:2712–2726.
- Scheffzek K, et al. (1997) The Ras-RasGAP complex: Structural basis for GTPase activation and its loss in oncogenic Ras mutants. *Science* 277:323–338.
- Jensen TR, et al. (2003) Water in contact with extended hydrophobic surfaces: Direct evidence of weak dewetting. *Phys Rev Lett* 90:086101.086101–086101.086104.
- Pasqualato S, Cherfils J (2005) Crystallographic evidence for substrate-assisted GTP hydrolysis by a small GTP binding protein. *Structure* 13:533–540.
- Boriack-Sjodin PA, Margarit SM, Bar-Sagi D, Kuriyan J (1998) The structural basis of the activation of Ras by Sos. *Nature* 394:337–343.
- Sullivan SM, Mishra R, Neubig RR, Maddock JR (2000) Analysis of guanine nucleotide binding and exchange kinetics of the *Escherichia coli* GTPase Era. *J Bacteriol* 182:3460–3466.
- Srivastava AK, Schlessinger D (1990) Mechanism and regulation of bacterial ribosomal RNA processing. *Annu Rev Microbiol* 44:105–129.
- Inoue K, Alsina J, Chen J, Inouye M (2003) Suppression of defective ribosome assembly in a rbfA deletion mutant by overexpression of Era, an essential GTPase in *Escherichia coli*. *Mol Microbiol* 48:1005–1016.
- Li Z, Pandit S, Deutscher MP (1999) RNase G (CafA protein) and RNase E are both required for the 5' maturation of 16S ribosomal RNA. *EMBO J* 18:2878–2885.
- Kaczanowska M, Ryden-Aulin M (2007) Ribosome biogenesis and the translation process in *Escherichia coli*. *Microbiol Mol Biol Rev* 71:477–494.
- Thammana P, Held WA (1974) Methylation of 16S RNA during ribosome assembly in vitro. *Nature* 251:682–686.
- Connolly K, Rife JP, Culver G (2008) Mechanistic insight into the ribosome biogenesis functions of the ancient protein KsgA. *Mol Microbiol* 70:1062–1075.
- Desai PM, Rife JP (2006) The adenosine dimethyltransferase KsgA recognizes a specific conformational state of the 30S ribosomal subunit. *Arch Biochem Biophys* 449:57–63.
- Komarova AV, Tchufistova LS, Supina EV, Boni IV (2002) Protein S1 counteracts the inhibitory effect of the extended Shine-Dalgarno sequence on translation. *RNA* 8:1137–1147.
- Wilson DN, Nierhaus KH (2005) Ribosomal proteins in the spotlight. *Crit Rev Biochem Mol Biol* 40:243–267.
- Chen X, Chen S-M, Powell B, Court DL, Ji X (1999) Purification, characterization and crystallization of ERA, an essential GTPase from *Escherichia coli*. *FEBS Lett* 445:425–430.